

# Automatic detection and prediction of nAMD activity change in retinal OCT using Siamese networks and Wasserstein Distance for ordinality

Taha Emre<sup>1\*</sup>, Teresa Araújo<sup>2\*</sup>, Marzieh Oghbaie<sup>2\*</sup>, Dmitrii Lachinov<sup>2</sup>,  
Guilherme Aresta<sup>2</sup>, and Hrvoje Bogunović<sup>2</sup>

<sup>1</sup> Dept. of Ophthalmology and Optometry, Medical University of Vienna, Austria

<sup>2</sup> Christian Doppler Laboratory for Artificial Intelligence in Retina, Institute of Artificial Intelligence, Center for Medical Data Science, Medical University of Vienna, Austria

**Abstract.** Neovascular age-related macular degeneration (nAMD) is a leading cause of vision loss among older adults, where disease activity detection and progression prediction are critical for nAMD management in terms of timely drug administration and improving patient outcomes. Recent advancements in deep learning offer a promising solution for predicting changes in AMD from optical coherence tomography (OCT) retinal volumes. In this work, we proposed deep learning models for the two tasks of the public MARIO Challenge at MICCAI 2024, designed to detect and forecast changes in nAMD severity with longitudinal retinal OCT. For the first task, we employ a Vision Transformer (ViT) based Siamese Network to detect changes in AMD severity by comparing scan embeddings of a patient from different time points. To train a model to forecast the change after 3 months, we exploit, for the first time, an Earth Mover (Wasserstein) Distance-based loss to harness the ordinal relation within the severity change classes. Both models ranked high on the preliminary leaderboard, demonstrating that their predictive capabilities could facilitate nAMD treatment management.\*\*

**Keywords:** Longitudinal change detection · Age-related macular edema · Siamese networks · Ordinal classification.

## 1 Introduction

Neovascular age-related macular degeneration (nAMD) is a progressive exudative disease characterized by the accumulation of fluid in the macula, which can significantly impair vision function [6]. Anti-VEGF treatments have shown great efficacy in mitigating AMD progression, and the positive effects are optimized by reducing the time from fluid onset to treatment, and thus regular follow-up is crucial for successful patient outcomes. The presence and extent of

---

\* These authors contributed equally to this work

\*\* <https://github.com/EmreTaha/Siamese-EMD-for-AMD-Change>

exudative signs, such as intraretinal and subretinal fluid, which are best visible on optical coherence tomography (OCT) images, are relevant markers for anti-VEGF administration [19]. Thus, predicting and accurately detecting changes in neovascularization activity are pivotal tasks for treatment management. The "Monitoring Age-related Macular Degeneration Progression In Optical Coherence Tomography" (MARIO) Challenge, organized as part of MICCAI 2024 [1], aims the development of automatic methods for nAMD progression assessment and evolution prediction.

### 1.1 Longitudinal change detection in retinal OCT

The manual assessment of changes between image pairs is time-consuming and challenging, highlighting the need for automated systems to detect meaningful changes and reduce specialists' workload. Although machine learning, particularly deep learning, has advanced in automating OCT disease diagnostics, there has been little focus on detecting changes between sequential OCT images.

In medical image analysis, current deep learning methods for change detection usually fall into two categories: 1) Siamese networks [13,12,21], or 2) Graph-based methods [9,18]. In Li *et al.* [13], change detection is approached as a metric-learning problem, using a Siamese neural network to assess changes between two patient visits. A contrastive loss function is applied between features of two images, labeled as *change* or *no change*, to output a pairwise distance between images from two time points. This method was tested on retinal photographs (diabetic retinopathy of prematurity) and knee x-rays (osteoarthritis). In Li *et al.* [12], the same authors used a similar approach to track COVID-19 pulmonary disease severity in chest x-rays.

In contrast, Karward *et al.* [9] proposed a graph-based, anatomy-aware model for tracking changes between chest X-rays by using both local and global anatomical information. This model provides localized comparisons between sequential X-ray images and outperformed Siamese-based models. However, this type of approach is more suitable when the structures are within a rigid region, and thus have a stable anatomical location (e.g., chest x-rays), and are not that suitable for retinal OCT, where pathologies can cause significant tissue deformations.

### 1.2 Prediction of nAMD evolution within 3 months on OCT

nAMD severity change prediction is crucial for patient follow-up scheduling and timely drug (anti-VEGF) administration. In this aspect, it is essential to have a predictive model that can assess the change in AMD disease activity within a meaningful time-frame from an OCT scan acquired at a visit. Prior work has largely focused on a related task of intermediate AMD progression prediction [4,2,17,22]. The main challenge of training a predictive model of disease progression and treatment response is the training data. Since, the nature of the task is temporal, it is crucial to have follow-up visits from a patient to create a longitudinal dataset. In [4,2,17], they used longitudinal self-supervised learning methods to learn the temporal relations. Additionally, most of the available

OCTs have no observable change within short time windows, resulting in severe class imbalance, requiring specialized deep learning loss terms to address this [14].

### 1.3 Contributions

We contribute to the state of the art in longitudinal retinal OCT assessment in two ways. First, we propose a Siamese-based approach, SiamRETFound, relying on an OCT foundation model (RETFound [23]) and additional pretraining for learning to estimate clinically-relevant changes between two patient B-scans. Second, we propose a classifier model that predicts the nAMD evolution within 3 months. Specifically, our novel loss has 2 parts: a focal loss to address the severe class imbalance, and an Earth Mover’s Distance-based (EMD) loss to harness the ordinal relation within the severity change classes. To our knowledge, this is the first study to use EMD for predicting disease severity evolution.

### 1.4 MARIO Challenge

We assess our methods on the two tasks of the MARIO challenge. Task 1 (T1) aims at developing algorithms to classify changes in disease activity from pairs of retinal OCT B-scans from two visits of patients with nAMD undergoing anti-VEGF treatment, to support decision-making. The classification categories were *Reduced*, *Stable*, *Worsened*, or *Other* (Uninterpretable). Based on our qualitative assessment of the provided training set, *Other* seemed to be associated with scenarios that prevented proper clinical assessment, such as the presence of noise, obscured regions, vertical flipping of the scan, poor alignment between image pairs, etc. (Fig. 2: (e)-(g)). However, no objective criteria was provided, and there were a few nuanced cases (Fig. 2: (g)).

In Task 2 (T2), the goal is to train a predictive model that can accurately predict the change in disease activity within 3 months, given a single B-scan. The prediction categories are *Reduced*, *Stable* and *Worsened*. Even though the labels and the prediction are on B-scan level, labels are consistent within a volume.

## 2 Method

### 2.1 T1: SiamRETFound for longitudinal change detection

We propose SiamRETFound, a Siamese neural network with shared weights for evaluating change between retinal B-scans from two visits of the same patient (Fig. 1). SiamRETFound uses a late fusion approach by extracting and concatenating two feature representations, one for each B-scan. The resulting feature vector, which integrates meaningful features from both time points, is then processed by a classification head to obtain the change detection. Ultimately, SiamRETFound learns to assess which differences between the extracted features are relevant to identify clinically meaningful changes.

The backbone for feature extraction consists of a pair encoders of the RETFound model, a foundation model pre-trained on retinal OCTs using a masked autoencoder strategy [23]. The encoder is a large vision Transformer (ViT) with 24 Transformer blocks and embedding vector size of 1024. The classification head has a fully connected (FC) layer with 256 neurons and a ReLU activation, 25% dropout, and a FC with 4 output neurons (number of classes).

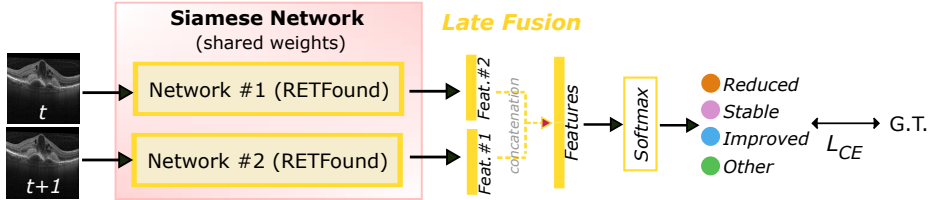


**Fig. 1.** SiamRETFound approach for longitudinal change detection in retinal OCT.

The full siamese network is first pretrained on a public OCT dataset using a simulated binary change detection task: *change/no change*. The network is then finetuned on the MARIO training data for classification of the target classes.

**Datasets and Evaluation** For training and evaluating our model we used the MARIO challenge task 1 development data. This is composed of a training set for which ground truth labels are provided and a validation set for which labels are kept hidden and that is used for ranking participants. The training set 14496 has B-scan pairs from 68 patients, with up to 10 visits per patient. The validation set has 7010 pairs from 34 patients. All OCT volumes were acquired with Spectralis device and longitudinal 3D volumes were anatomically aligned with the follow-up mode from the device.

The public Kermamy dataset [10] used for pretraining consists of 100,000 images from patients belonging to one of the following classes: healthy, intermediate AMD, nAMD, and diabetic macular edema (DME). Surrogate binary labels *change/no change* were inferred from the disease classes: if both images have the same disease, the pair was attributed to *no change*, otherwise to *change*.

The evaluation metrics reported in this work include the official MARIO challenge metrics: F1-score (micro-averaging), Specificity and Rk-correlation coefficient (i.e., Mathews correlation coeff. for multiclass setting), along with Balanced accuracy and Cohen’s Kappa Coefficient ( $k$ ) that we added.

**Training details** The MARIO challenge training set was split patient-wise in 90% for training and 10% for validation. To generate the pretraining data from the Kermamy dataset, random pairs are taken from the original dataset, for a total of 300,000 image pairs. Both pretraining and finetuning follow the

same scheme. Training-time image augmentation is applied, ensuring the same augmentation on both images of a pair. Augmentations include resize-crop (minimum of 85% image size), rotation (up to 15°) and horizontal flipping. Images are resized to 224×224 pixels and the intensities are normalized by the ImageNet mean and standard deviation. Batches are balanced class-wise during training to compensate for the class imbalance. A warm-up is done in the beginning of the training with classification neurons frozen for 50 epochs. The Adam optimizer with an initial learning rate (LR) of 0.001 with an exponential decay was used, and the training loss was the cross-entropy loss. SiamRETFound was finetuned for up to 100 epochs with early stopping based on the average of the challenge evaluation metrics on the held out validation set.

**Ensembling** For the MARIO challenge ranking specifically, we used an ensembling strategy by combining the prediction probabilities of 10 different models: 1) 5 SiamRETFound-based models (with different training settings: optimizers, LR, augmentation schemes); 2) 5 Shifted WINDows (SWIN)[15] transformer-based models (5 folds). To obtain a prediction for a test image we took the mean of all models’ predictions per class, and chose the class with the maximum-score.

In our SWIN-based models, we first trained a SWIN transformer sequentially on three publicly available OCT datasets: OCTID [5], OCTDL [11], and Kermany [10]. Second, we finetuned the model for multi-label biomarker detection using the OLIVES dataset [16]<sup>3</sup>. This method ensures that the model is exposed to a broad spectrum of diseases, enhancing its ability to detect critical biomarkers in B-scans, crucial for change detection.

## 2.2 T2: WASSERSTEIN distance for RetInal disease Ordinality modeling (WARIO)

Our solution to T2 has 3 main components: masked-autoencoder based pretraining, finetuning with a novel approach to ordinal classes, and postprocessing to ensure volume level consistency based on individual B-scan level predictions.

*Pretraining* Pretraining is an important step of the current deep learning pipeline. In AMD disease progression tasks, numerous works showed the benefit of pretraining [2,4]. Recently, masked auto-encoders [7] (MAE) achieved the state-of-the-art in vision tasks. Following this trend, we pretrain our models with MAE by masking 75% of B-scans (Fig. 6) from a combined dataset of T1 and T2.

*Finetuning* Addressing T2 effectively requires accounting for (i) the class imbalance due to large number of *Stable*, and (ii) the ordinal relationship between the classes (*Reduced-Stable-Worsened*). While the class imbalance poses a challenge, the ordinality provides an opportunity for additional training signal. For the class

<sup>3</sup> Same splits as the IEEE SPS VIP Cup 2023: Ophthalmic Biomarker Detection.

imbalance, we adapted Focal Loss [14], which dynamically calculates weights for hard and easy examples, so that hard to classify samples will contribute more:

$$\ell_{\text{focal}} = -\alpha \sum_{i=0}^{C-1} y_i (1 - \hat{p}_i)^\gamma \log(\hat{p}_i), \quad (1)$$

where  $C$  is the number of classes, and  $\gamma$  is the focusing hyper-parameter for hard to classify samples. Additionally we undersample the majority class (*Stable*) during finetuning.

For the ordinality we use discrete earth-mover’s distance [8,20] (EMD, also known as Wasserstein-distance). Unlike the cross-entropy loss, it takes inter-class relations (e.g. ranking) into account when calculating the loss. In T2, the classes are ordered by their definition, as *Reduced-Stable-Worsened*. EMD calculates cumulative mass need to be moved to make one distribution similar to another:

$$\ell_{\text{EMD}} = \left( \frac{1}{C} \sum_{i=0}^{C-1} |\text{CDF}_y(i) - \text{CDF}_{\hat{p}}(i)|^2 \right)^{1/2}, \quad (2)$$

where  $\text{CDF}_p()$  is the cumulative distribution function calculated from the class probabilities or one-hot encoded target vector. The final training loss is the combination of these two loss terms with equal weighting.

*Postprocessing (Ensembling)* After pretraining and finetuning on 3-fold splits, the predictions are ensembled as follows. We make a single prediction from different training split folds in a B-scan level, and then an eye level prediction from available B-scans of a particular OCT volume. In general, the trained networks tend to predict *Stable* due to the imbalance. In order to alleviate this, the final prediction from the 3 outputs is set to class *Stable* if only all 3 models predict *Stable*, otherwise it is set to the majority vote.

In T2, the labels are provided at the OCT volume level, i.e. B-scans from a particular visit scan of a patient have the same label. To ensure this consistency in our predictions, we apply a majority voting. In order to avoid only predicting the majority *Stable* class, a volume level label is set to *Stable* if at least 80% (the class ratio) of the B-scan level predictions are *Stable*. If not, volume level label is the majority prediction. Then we set all B-scans of that volume to a single label, and reported the predictions in this manner.

**Datasets and Evaluation** T2 training data consisted of 8082 B-scans from 330 volumes for 61 patients. The provided validation split contained 3822 B-scans from 163 volumes for 29 patients. All OCT volumes are Spectralis and consecutive 3D volumes are registered. For metrics, the official MARIO challenge metrics: F1-score (micro-averaging), Specificity, Quadratic-weighted Kappa and Rk-correlation coefficient, and additional Balanced accuracy are used.

**Training details** We use ViT [3] base model with a single FC prediction head. It has 12 MHSA blocks with 12 parallel heads, embedding size of 768 and  $16 \times 16$  patch size. The prediction head uses global average pooled embedding features instead of the CLS token. We first run MAE pretraining for 800 epochs with a decayed LR of  $3E-4$ , weight decay of  $1E-2$ , and batch size of 256. We use AdamW as the optimizer with its Beta2 hyperparameter set to 0.95. We then finetune end-to-end for 200 epochs with a warm-up of 20 epochs, a LR of  $2.5E-4$  and a weight decay of  $1E-4$ . We used AdamW as the optimizer with Beta2 of 0.999. We only use 2D B-scans and considered each B-scan i.i.d (even from the same patient) during training. Training augmentations include translation, small rotation, and horizontal flipping. Each image is resized to  $224 \times 224$  pixels.

### 3 Results and Discussion

#### 3.1 T1: Longitudinal change detection

We showed that SiamRETFound is able to correctly classify longitudinal change for the majority of the OCT pairs (Table 1). The model is able to capture very subtle changes (Fig. 2: (a),(b)). Specifically for the change classes (*Reduced*, *Stable* and *Worsened*), which can be interpreted as an ordinal classification problem, we verified most errors occur between neighboring classes and little *Reduced/Worsened* cases are confounded (Appendix - Fig. 3). For the class *Other*, the majority of the confusion occurs with *Stable*, which can be attributed to the not so clear definition of *Other* (e.g., how much noise or obscured area constitutes an uninterpretable pair) (Fig. 2: (g)).

The occlusion sensitivity maps (Appendix - Fig. 5) suggest that the SiamRETFound model is capturing relevant features to classify change between image pairs, mostly focusing on fluid regions.

Despite SiamRETFound approach being better in terms of overall classification performance (inferred by the confusion matrix and the balanced accuracy and  $k$  metrics), concerning the MARIO challenge metrics the ensemble version outperformed the single model prediction. On the challenge leaderboard in the development phase we ranked 4<sup>th</sup> considering the mean of the evaluation metrics, with a score of 0.801 (scores of the top 3 teams: 0.828/0.805/0.804).

#### 3.2 T2: Prediction of AMD evolution within 3 months

In Task 2, the goal is to detect the change in AMD severity in 3 months from a provided past visit scan. We found that, it is crucial to have a strong pretraining step and correct loss terms. Only the combination of focal loss and EMD loss (WARIO) prevent the network from only predicting the *Stable* class. In Table 1, it is clear that WARIO is still heavily biased towards the majority class, highlighting the importance of a postprocessing step. Clinically we know that AMD change is a OCT volume level assessment from which we concluded that the B-scan level predictions need to be consistent along an OCT volume. We enforced

**Table 1.** Results of our methods in the MARIO challenge validation sets for T1 and T2. For T1, Kappa is Cohen’s Kappa; for T2, it is Quadratic-weighted Kappa.

Metric	Task 1 (T1)		Task 2 (T2)	
	SiamRETFound	Ensemble	WARIO	Ensemble
Balanced Acc.	0.713	0.691	0.336	0.485
Kappa <sup>T2</sup>	0.642	0.656	0.133	0.223
F1 Score <sup>T1,T2</sup>	0.817	0.833	0.720	0.705
Rk-Correlation <sup>T1,T2</sup>	0.642	0.657	0.004	0.206
Specificity <sup>T1,T2</sup>	0.917	0.911	0.666	0.722
Average <sup>(*)</sup>	0.792	0.801	0.351	0.469

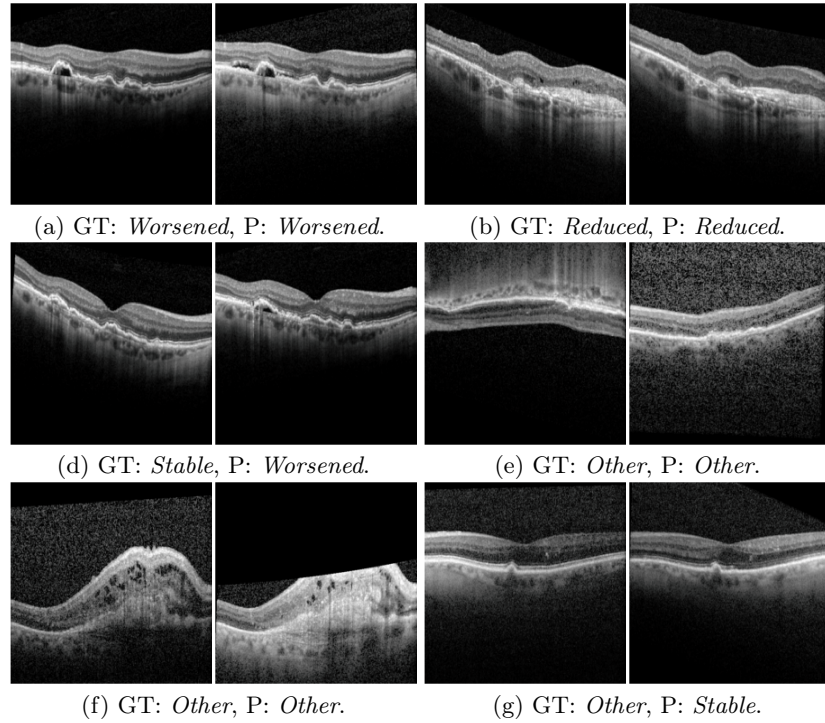


**Fig. 2.** Examples of SiamRETFound predictions (GT: ground truth, P: prediction).

this consistency in the postprocessing step combined with an ensemble of 3-fold data split. Even though F1-score dropped slightly, WARIO improved along other metrics. It is important to highlight that postprocessing improved Rk-correlation the most which is generally used in imbalanced classification problems. At the end, WARIO ranked 2<sup>nd</sup> in the challenge leaderboard.



## 4 Conclusions

MICCAI'24 MARIO challenge aims to model AMD severity change in 2 setups: (i) predicting the change by comparing B-scans from two time points, (ii) predicting the change after 3 months from a single B-scan. We proposed SiamRET-Found, a siamese-based approach that was able to effectively classify longitudinal change in OCT pairs, even for very subtle cases. The proposed model captured relevant features to classify change between B-scan pairs, mostly focusing on exudative regions. Predicting the change in OCTs from a single past visit is extremely challenging task. Our method, WARIO, uses focal loss for class imbalance and EMD loss to exploit ordinal relation in the severity change classes, preceded by a strong MAE based pretraining. The proposed methods show potential to facilitate the clinical workflow on nAMD diagnosis from retinal OCTs and allow timely and thus more effective treatment planning.

## References

1. MARIO challenge (8 2024), <https://www.codabench.org/competitions/2852>
2. Chakravarty, A., Emre, T., Leingang, O., Riedl, S., Mai, J., Scholl, H.P., Sivaprasad, S., Rueckert, D., Lotery, A., Schmidt-Erfurth, U., et al.: Morph-ssl: Self-supervision with longitudinal morphing for forecasting amd progression from oct volumes. *IEEE Transactions on Medical Imaging* (2024)
3. Dosovitskiy, A., Beyer, L., Kolesnikov, A., Weissenborn, D., Zhai, X., Unterthiner, T., Dehghani, M., Minderer, M., Heigold, G., Gelly, S., Uszkoreit, J., Houlsby, N.: An image is worth 16x16 words: Transformers for image recognition at scale. In: *International Conference on Learning Representations* (2021)
4. Emre, T., Chakravarty, A., Rivail, A., Riedl, S., Schmidt-Erfurth, U., Bogunović, H.: Tinc: Temporally informed non-contrastive learning for disease progression modeling in retinal oct volumes. In: *International Conference on Medical Image Computing and Computer-Assisted Intervention*. pp. 625–634. Springer (2022)
5. Gholami, P., Roy, P., Parthasarathy, M.K., Lakshminarayanan, V.: Octid: Optical coherence tomography image database. *Computers & Electrical Engineering* **81**, 106532 (2020)
6. Guymer, R.H., Campbell, T.G.: Age-related macular degeneration. *The Lancet* **401**(10386), 1459–1472 (2023)
7. He, K., Chen, X., Xie, S., Li, Y., Dollár, P., Girshick, R.: Masked autoencoders are scalable vision learners. In: *Proceedings of the IEEE/CVF conference on computer vision and pattern recognition*. pp. 16000–16009 (2022)
8. Hou, L., Yu, C.P., Samaras, D.: Squared earth mover’s distance-based loss for training deep neural networks. *arXiv preprint arXiv:1611.05916* (2016)
9. Karwande, G., Mbakwe, A.B., Wu, J.T., Celi, L.A., Moradi, M., Lourentzou, I.: CheXRelNet: An Anatomy-Aware Model for Tracking Longitudinal Relationships Between Chest X-Rays. *Lecture Notes in Computer Science (including sub-series Lecture Notes in Artificial Intelligence and Lecture Notes in Bioinformatics)* **13431**, 581–591 (2022). [https://doi.org/10.1007/978-3-031-16431-6\\_55](https://doi.org/10.1007/978-3-031-16431-6_55)
10. Kermany, D.S., Goldbaum, M., Cai, W., et al.: Identifying Medical Diagnoses and Treatable Diseases by Image-Based Deep Learning. *Cell* **172**(5), 1122–1131 (2018). <https://doi.org/10.1016/j.cell.2018.02.010>

11. Kulyabin, M., Zhdanov, A., Nikiforova, A., Stepichev, A., Kuznetsova, A., Ronkin, M., Borisov, V., Bogachev, A., Korotkich, S., Constable, P.A., et al.: Octdl: Optical coherence tomography dataset for image-based deep learning methods. *Scientific Data* **11**(1), 365 (2024)
12. Li, M.D., Arun, N.T., Gidwani, M., Chang, K., Deng, F., Little, B.P., Mendoza, D.P., Lang, M., Lee, S.I., O'Shea, A., Parakh, A., Singh, P., Kalpathy-Cramer, J.: Automated assessment and tracking of COVID-19 pulmonary disease severity on chest radiographs using convolutional siamese neural networks. *Radiology: Artificial Intelligence* **2**(4), 1–39 (2020). <https://doi.org/10.1148/ryai.2020200079>
13. Li, M.D., Chang, K., Bearce, B., Chang, C.Y., Huang, A.J., Campbell, J.P., Brown, J.M., Singh, P., Hoebel, K.V., Erdoğmuş, D., Ioannidis, S., Palmer, W.E., Chiang, M.F., Kalpathy-Cramer, J.: Siamese neural networks for continuous disease severity evaluation and change detection in medical imaging. *npj Digital Medicine* **3**(1), 1–9 (2020). <https://doi.org/10.1038/s41746-020-0255-1>
14. Lin, T.Y., Goyal, P., Girshick, R., He, K., Dollár, P.: Focal loss for dense object detection. In: *Proceedings of the IEEE international conference on computer vision*. pp. 2980–2988 (2017)
15. Liu, Z., Lin, Y., Cao, Y., Hu, H., Wei, Y., Zhang, Z., Lin, S., Guo, B.: Swin transformer: Hierarchical vision transformer using shifted windows. In: *Proceedings of the IEEE/CVF international conference on computer vision*. pp. 10012–10022 (2021)
16. Prabhushankar, M., Kokilepersaud, K., Logan, Y.y., Trejo Corona, S., AlRegib, G., Wykoff, C.: Olives dataset: Ophthalmic labels for investigating visual eye semantics. *Advances in Neural Information Processing Systems* **35**, 9201–9216 (2022)
17. Rivail, A., Schmidt-Erfurth, U., Vogl, W.D., Waldstein, S.M., Riedl, S., Grechenig, C., Wu, Z., Bogunovic, H.: Modeling disease progression in retinal OCTs with longitudinal self-supervised learning. In: *Predictive Intelligence in Medicine: Second International Workshop, PRIME 2019, Held in Conjunction with MICCAI 2019, Shenzhen, China, October 13, 2019, Proceedings 2*. pp. 44–52. Springer (2019)
18. Rochman, S., Szeskin, A., Lederman, R., Sosna, J., Joskowicz, L.: Graph-based automatic detection and classification of lesion changes in pairs of CT studies for oncology follow-up. *International Journal of Computer Assisted Radiology and Surgery* (2023). <https://doi.org/10.1007/s11548-023-03000-2>
19. Schmidt-Erfurth, U., Waldstein, S.M.: A paradigm shift in imaging biomarkers in neovascular age-related macular degeneration. *Progress in Retinal and eye Research* **50**, 1–24 (2016)
20. Talebi, H., Milanfar, P.: Nima: Neural image assessment. *IEEE transactions on image processing* **27**(8), 3998–4011 (2018)
21. To, M.S., Sarno, I.G., Chong, C., Jenkinson, M., Carneiro, G.: Self-Supervised Lesion Change Detection and Localisation in Longitudinal Multiple Sclerosis Brain Imaging. *Lecture Notes in Computer Science (including subseries Lecture Notes in Artificial Intelligence and Lecture Notes in Bioinformatics)* **12907 LNCS**, 670–680 (2021). [https://doi.org/10.1007/978-3-030-87234-2\\_63](https://doi.org/10.1007/978-3-030-87234-2_63)
22. Yim, J., Chopra, R., Spitz, T., Winkens, J., Obika, A., Kelly, C., Askham, H., Lukic, M., Huemer, J., Fasler, K., et al.: Predicting conversion to wet age-related macular degeneration using deep learning. *Nature Medicine* **26**(6), 892–899 (2020)
23. Zhou, Y., Chia, M.A., Wagner, S.K., et al.: A foundation model for generalizable disease detection from retinal images. *Nature* **622**(7981), 156–163 (2023). <https://doi.org/10.1038/s41586-023-06555-x>

## A Appendix

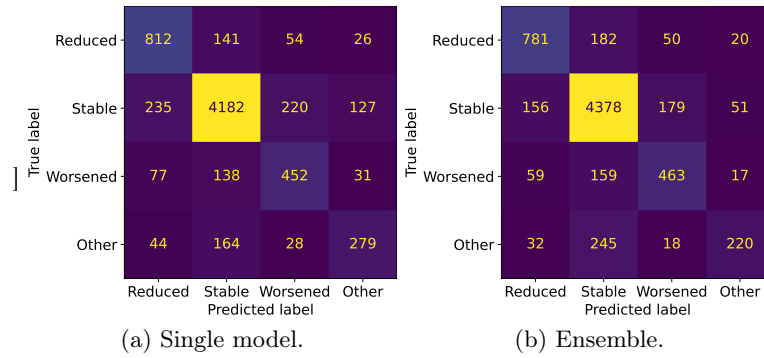


**Fig. 3.** Confusion matrices for Longitudinal change detection (MARIO Task 1).

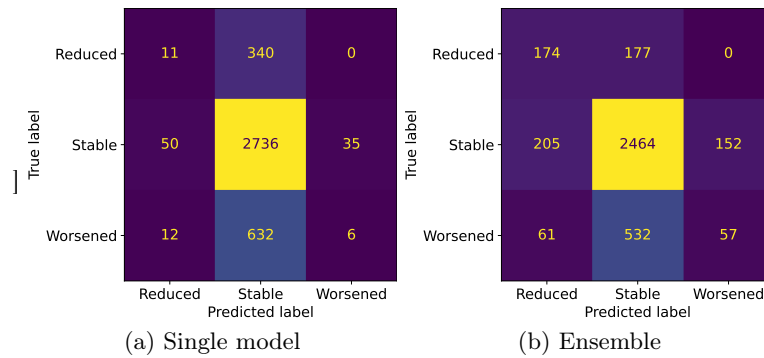


**Fig. 4.** Confusion matrices for AMD evolution prediction (MARIO Task 2)

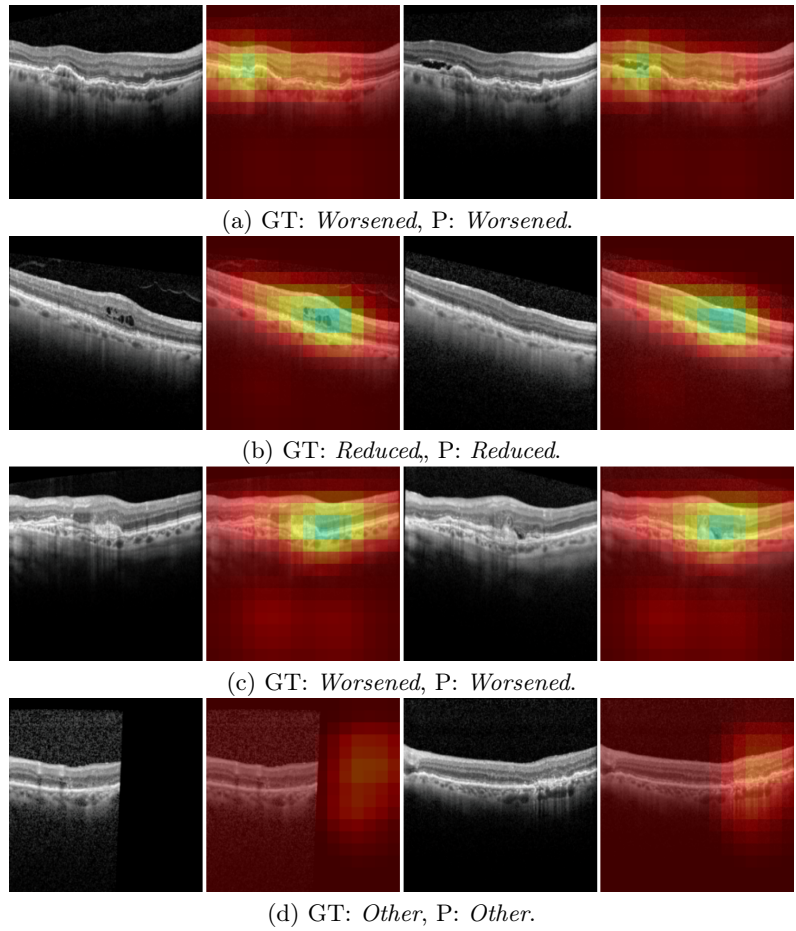


**Fig. 5.** Occlusion map sensitivity. Map values are from 0 (blue) to 1 (red). Lower values indicate the occluded region impacted more the final prediction.

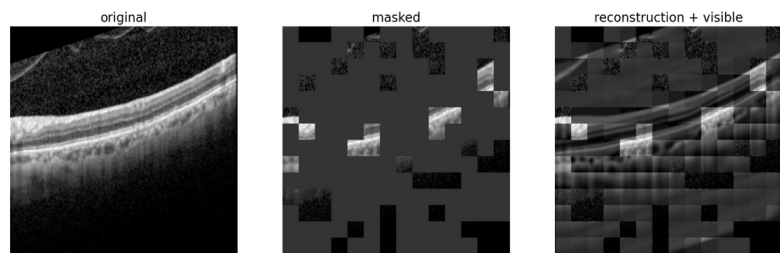


**Fig. 6.** MAE pretraining with masking and reconstruction.